Polymer-based nanoparticles loaded with a TLR7 ligand to target the lymph node for immunostimulation

Jérôme Widmer[a], Cédric Thauvin[b], Inès Mottas[a,b], Van Nga Nguyen[b], Florence Delie[b], Eric Allémann[b,*], Carole Bourquin[a,b,**]

[a] Department of Medicine, Faculty of Science, University of Fribourg, Chemin Du Musée 5, 1700 Fribourg, Switzerland
[b] School of Pharmaceutical Sciences, University of Geneva, University of Lausanne, Rue Michel-Servet 1, 1211 Geneva, Switzerland

A R T I C L E   I N F O

A B S T R A C T

Small-molecule agonists for the Toll-like receptors (TLR) 7 and 8 are effective for the immunotherapy of skin cancer when used as topical agents. Their systemic use has however been largely unsuccessful due to dose-limiting toxicity. We propose a polymer-based nanodelivery system to target resiquimod, a TLR7 ligand, to the lymph node in order to focus the immunostimulatory activity and to prevent a generalized inflammatory response. We demonstrate successful encapsulation of resiquimod in methoxypoly(ethylene glycol)-b-poly(DL-lactic acid) (mPEG-PLA) and mixed poly(DL-lactic-co-glycolic acid) (PLGA)/mPEG-PLA nanoparticles. We show that these particles are taken up mainly by dendritic cells and macrophages, which are the prime initiators of anticancer immune responses. Nanoparticles loaded with resiquimod activate these cells, demonstrating the availability of the immune-stimulating cargo. The unloaded particles are non-inflammatory and do not have cytotoxic activity on immune cells. Following subcutaneous injection in mice, mPEG-PLA and PLGA/mPEG-PLA nanoparticles are detected in dendritic cells and macrophages in the draining lymph nodes, demonstrating the targeting potential of these particles. Thus, polymer-based nanoparticles represent a promising delivery system that allows lymph node targeting for small-molecule TLR7 agonists in the context of systemic cancer immunotherapy.

1. Introduction

Chemotherapy, radiotherapy and surgery have long formed the mainstay of cancer treatment, but new therapies such as immunotherapy are emerging. This strategy, which is based on the stimulation of the patient's own immune system against tumor tissues, has proven highly successful in different types of cancer. The initiation of an anticancer immune response is orchestrated by cells of the immune system, in particular macrophages and dendritic cells. These cell types are activated through triggering of pattern-recognition receptors such as the family of Toll-like receptors (TLRs), which are pivotal for the generation of many types of immune responses. TLRs play a key role in immunotherapy, as they participate in the induction of an innate immune response that controls the development of antitumoral immunity (Iwasaki and Medzhitov, 2015).

Imiquimod and resiquimod (R848), two synthetic imidazoquinolines, activate signaling of TLR7 and TLR8 (Heil et al., 2003). These receptors are mainly expressed by monocytes, macrophages and dendritic cells and are localized intracellularly in the endosomal membranes (Nishiya and DeFranco, 2004). Activation of TLR7 leads to development of NK-cell and cytotoxic T-cell responses, which are instrumental for anticancer immunity, and at the same time blocks the function of immunosuppressive cells such as regulatory T cells and myeloid-derived suppressor cells (Anz et al., 2010; Bourquin et al., 2009; Dumitru et al., 2009; Hotz et al., 2016; Spinetti et al., 2016).

Due to their proven clinical efficacy for the topical treatment of skin tumors (Papakostas and Stockfleth, 2015), imidazoquinolines have been attractive candidates as immunostimulating agents for systemic use in the treatment of non-skin cancers. Unfortunately, systemic administration has met with limited success in clinical trials so far (Iribarren et al., 2016). Part of the lack of efficacy may lie in a phenomenon of tolerance that leads to immune unresponsiveness upon repetitive applications of these TLR7 ligands (Bourquin et al., 2011). In addition, upon systemic application in clinical studies, dose-limiting toxicity restricted the therapeutic potential of these drugs (Kobold et al., 2014). The lack of solubility of these molecules in aqueous media

---

* Corresponding author.
** Corresponding author at: School of Pharmaceutical Sciences, University of Geneva, University of Lausanne, Rue Michel-Servet 1, 1211 Geneva, Switzerland.
E-mail addresses: eric.allemann@unige.ch (E. Allémann), carole.bourquin@unige.ch (C. Bourquin).

may also represent a hurdle for their development as systemic treatments (Allémann et al., 1993; Fahr and Liu, 2007).

The development of polymer nanoparticles encapsulating TLR7 ligands may bypass their limitations for systemic application. The targeting of the immune activating substances by particulate delivery directly to the lymph nodes, where the anticancer immune response is initiated, could help reduce unspecific adverse effects (Kranz et al., 2016). Furthermore, encapsulation in a polymer matrix allows the formulation of poorly hydrophilic drugs as injectable suspensions and may provide a delayed release to avoid tolerance (Leroux et al., 1996; Zeisser-Labouèbe et al., 2006). To date, a limited number of studies have reported the use of nanocarriers in imiquimod or resiquimod delivery for cancer immunotherapy. Poly(DL-lactic-co-glycolic acid) (PLGA) particles containing a TLR7 agonist combined with a vascular disruptive agent were administered intratumorally with good results (Seth et al., 2017). In a clinical study, imiquimod and a TLR9 agonist coupled with a peptide antigen were loaded into virus-like nanoparticles and administered as intralymph node injection (Goldinger et al., 2012). The co-encapsulation of TLR3 and TLR7 ligands and antigen in PLGA nanoparticles has been reported as vaccine design and enhances the development of B cell responses (Kasturi et al., 2011).

An ideal system in nanomedicine should improve the activity of drugs while decreasing adverse effects by a precise delivery to target tissues (Riehemann et al., 2009). New delivery systems with optimized properties that include biocompatibility, favorable biodistribution, prolonged circulation time, optimal pharmacokinetics, and high loading capacity are thus currently under investigation. In the present report, resiquimod was encapsulated into pegylated polymer-based nanoparticles. Poly(DL-lactic acid) (PLA) and PLGA derivative polymers have been chosen for the matrix of the particles based on their well-known biocompatibility when used in implants or microspheres for injectable slow release delivery systems. These polymers have been approved by the FDA and numerous formulations are already on the market, for example Nutropin Depot®, Decapeptyl®, Trelstar™ Depot as microparticles or Zoladex®, as implant. Methoxypoly(ethylene glycol) (mPEG) residues have been added to avoid excessive and fast opsonization of the particles upon administration leading to a rapid elimination. The therapeutic aim for the resiquimod-loaded nanoparticles is to target the drug to dendritic cells and macrophages in the lymph node, since these cells are critical for the initiation of an antitumoral immune response. This directed delivery should support the development of anticancer immunity while at the same time reducing unwanted systemic proinflammatory reactions. This proof of concept study aims at demonstrating the possibility of encapsulating R848 in nanoparticles made of two polymers without losing or shielding the pharmacological efficiency of the active compound.

2. Materials and methods

2.1. Materials for NP synthesis

PLGA (RG 504-H) and mPEG-PLA polymers were either obtained from Boehringer Ingelheim or synthesized by ring-opening polymerization, respectively. 3,3′Dioctadecyl-oxacarbocyanine perchlorate (DiO), stannous octoate, methoxypolyethylene glycol 2000 (mPEG2000), sucrose and polyvinyl alcohol (PVAL) (Mowiol 4-88, 26000 Da, 88% hydrolysis) were all purchased from Sigma-Aldrich. DL-Lactide was purchased from Polysciences. Resiquimod was purchased from Enzo Life Sciences. All materials were used as received. The water was filtered through a Millipak 40 filter by a Millipore system.

2.2. Cell line and mice

The J774A.1 macrophage cell line (ATCC) was plated in complete medium: high glucose (4.5 g/l) DMEM (Biowest), 10% FCS (Biological industries) 2 mmol/ml L-glutamine (PAA), 1 nM sodium pyruvate (PAA), 0.5% ciproxin (Bayer) in flat-bottom 96-well plates at a concentration of 5×10^5 cells/ml (100 µl/well in a 96-well plate) unless indicated otherwise, and cultured at 37 °C in 5% CO_2.

C57BL/6 mice were purchased from Janvier Labs (Le Genest Saint Isle, France) and maintained in SPF conditions. Experiments were performed at 6–12 weeks of age. All experiments were performed in accordance with Swiss regulations on animal experimentation.

2.3. Synthesis of mPEG-PLA

After three successive vacuum-argon cycles a mixture of mPEG2000 (1.0 g, 0.5 mmol), DL-lactide (4.6 g, 40 mmol), and stannous octoate (7 mg) were stirred at 115 °C for 20 h under an argon atmosphere. The resulting mixture was then diluted in dry $CHCl_3$ and precipitated in cold and dry petroleum ether. After filtration, the crude polymer was dried under vacuum to give mPEG-PLA without any further purification. The chemical structure and molecular composition of mPEG-PLA diblock copolymer was determined by ^{1}H NMR spectroscopy. ^{1}H NMR (300 MHz, $CDCl_3$) δ ppm 5.29–5.09 (m, 100 H), 3.64 (s, 146 H), 3.38 (s, 3 H), 1.63–1.44 (m, 300 H).

2.4. Nanoparticle preparation

A solution of 150 mg of polymer (PLGA/mPEG-PLA 67/33 w/w: NPa or mPEG-PLA: NPb) in 1 ml of dichloromethane was emulsified in 2 ml of a 2.5% PVAL solution by ultra-sonication with a Branson Digital Sonifier (Branson Ultrasonics, Danbury, USA) for 40 s and with amplitude of 50%. The freshly prepared emulsion was then added dropwise to 50 ml of water and stirred 1 h at 1300 rpm with an Ultra-Turrax Eurostar digital Euros ST D (IKA-Werke GmbH & Co., Staufen, Germany) in an ice bath. The stirring speed was then reduced to 600 rpm and the solution was stirred for 2 h at room temperature to remove the solvent. 3 cycles of washing and centrifugation using an Avanti 30 Centrifuge (Beckman, USA) equipped with a F1010 Fixed-Angle Rotor (Beckman, USA), each time for 15 min at 34,000 × g, were finally done to obtain 10 ml of a nanoparticle suspension. The latter was then divided in five fractions of 2 ml in which 1 ml of a 15% w/w sucrose aqueous solution was added. The samples were freeze dried using a Christ Alpha 2-4 LD plus freeze dryer (Christ, Osterode am Harz, Germany). In this study, one cycle of 48 h was done at a pressure of 0.6 mBar and a temperature of − 85 °C, the final heating temperature was set to 22 °C. In the case of loaded nanoparticles, R848 (5 mg) or DiO (22.5 µg) were solubilized in dichloromethane and added to the polymer solution before mixing it with the PVA solution. Different types of NP were prepared, as presented in Table 1.

Table 1
Composition and characteristics of the different batches of NP.

NP	PLGA	mPEG-PLA	Loading	Size (PDI)	Drug loading µg/mg NP
R848-NPa	67%	33%	R848	278 nm (0.19)	8.36
R848-NPb	0	100%	R848	154 nm (0.14)	0.74
u-NPa	67%	33%	Ø	254 nm (0.10)	/
u-NPb	0	100%	Ø	176 nm (0.17)	/
DiO-NPa	67%	33%	DiO	230 nm (0.14)	/
DiO-NPb	0	100%	DiO	201 nm (0.16)	/
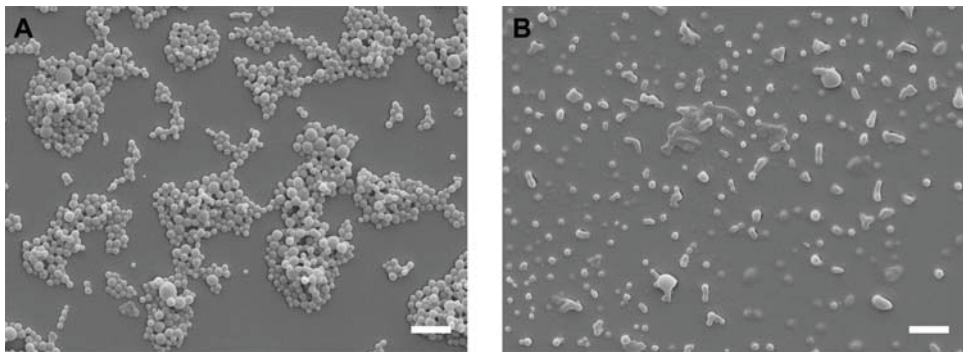
Fig. 1. Scanning electron microscopy images of (A) NPa and (B) NPb (scale bar = 1 μm).
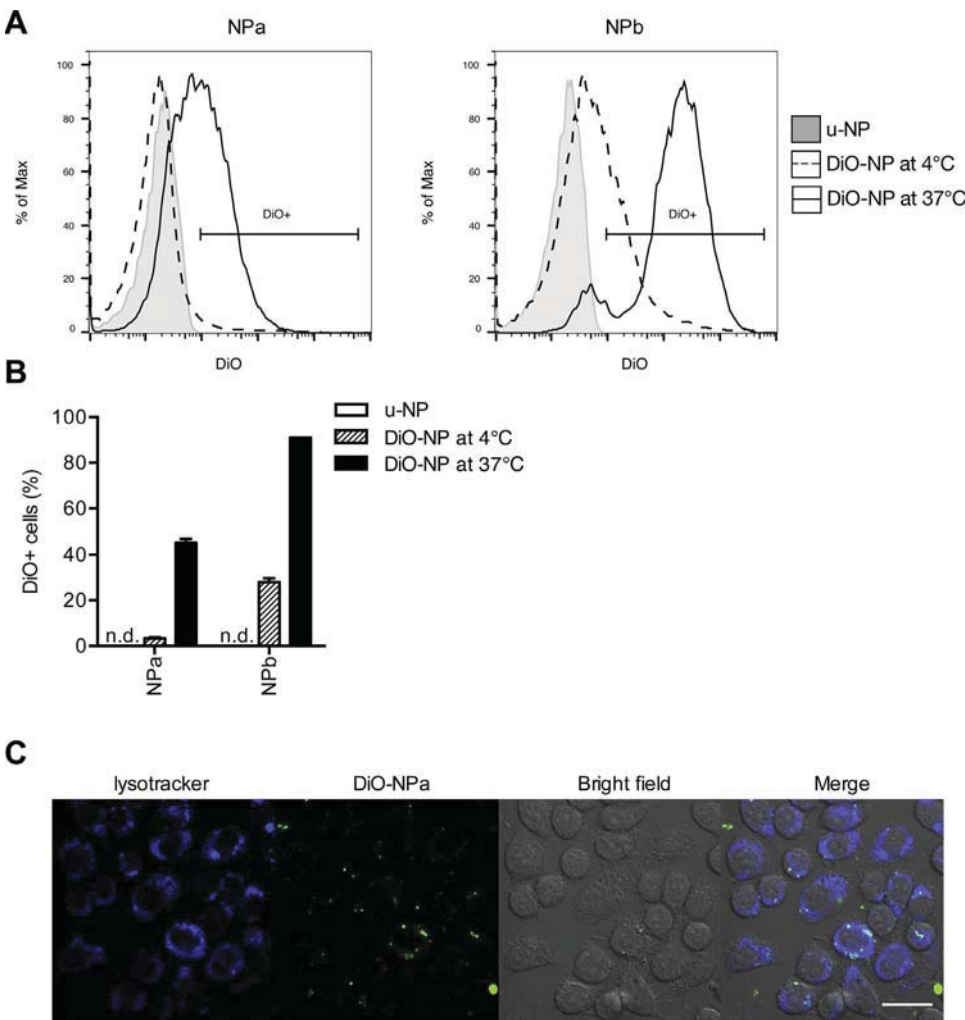
**Fig. 2.** NPa and NPb are efficiently taken up by macrophages.

(A–B) J774 macrophages were exposed for 24 h to DiO-NPa or DiO-NPb at 4 °C or 37 °C and the uptake was assessed by flow cytometry. (A) Representative histograms showing the intensity of DiO labeling. (B) Percentage of DiO-positive cells. Each bar represents mean ± SEM of one experiment performed in triplicate. Data are representative of 4 independent experiments. (C) J774 macrophages were exposed for 2 h to DiO-NPa and analyzed by confocal microscopy. Green: DiO-NPa; blue: Lysotracker. Pictures are representative of 5 independent experiments (scale bar = 33 μm). (For interpretation of the references to colour in this figure legend, the reader is referred to the web version of this article.)

2.5. Characterization of NP

NP size and ζ-potential were determined with a Zetasizer 3000 (Malvern Instruments, Ltd., U.K.) after dilution of nanoparticle suspensions in Milli-Q filtered water according to the supplier's recommendations: *ca.* 0.1 mg/ml to obtain a slightly opalescent suspension. NP morphology was determined by scanning electron microscopy (SEM) using a JSM-7001FA microscope (JEOL, Tokyo, Japan). A drop of nanoparticle suspension in water was placed onto stubs, dried under vacuum and covered with a 15–20 nm layer of gold. The stubs were then examined at emission 5.0 kV and working distance between 9.3 nm and 12.0 nm.

NP were dissolved in HPLC grade DMSO at a concentration of 3 mg/ml. The loaded amount of R848 was quantified by a U-HPLC separation performed by a Thermo Scientific Accela LC system equipped with a Thermo Scientific Accela PDA (Thermo Fischer Scientific, Waltham, USA). The column used was a C18 Hypersil Gold (50 × 2.1 mm, 1.9 μm particle size, 175 Å pore size; Thermo Fischer Scientific, Waltham, USA). The chromatographic separation was carried out with a linear gradient mode starting from 98% of water containing 0.1% of formic acid (1.8–4 min) to 98% of acetonitrile containing 0.1% of formic acid (for two minutes) with a flow rate of 400 μl/min. R848 was detected at 320 nm wavelength. The injection volume was 10 μl.
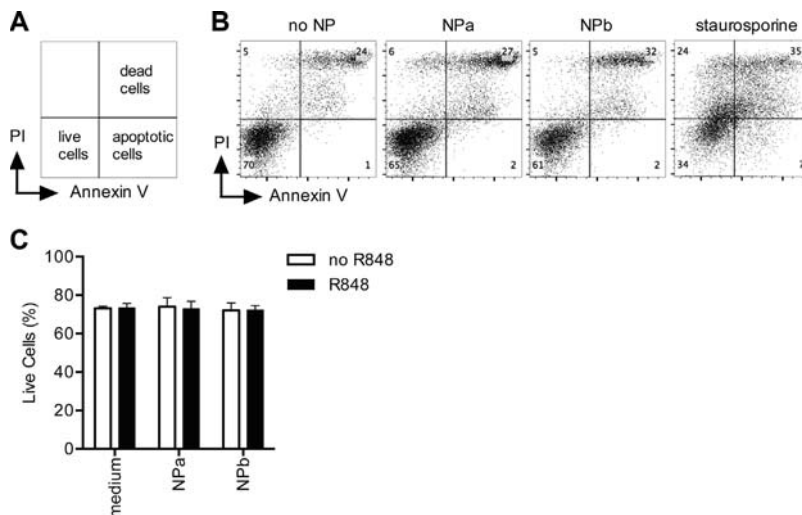
Fig. 3. NP do not affect cell viability.
J774 macrophages were exposed for 24 h to u-NP or R848-NP and viability was assessed by flow cytometry. (A and B) Representative dot plots, (C) percentage of Annexin V/PI double-negative cells (live cells). Medium: incubation condition without NP, without R848 (white bar) or with free R848 (black bar). Each bar represents mean ± SEM of 6 independent experiments performed in quadruplicate.

2.6. NP dilution for cell culture

Lyophilized NP were suspended in apyrogenic water at a concentration of 20 μg/ml R848 (200× working concentration). The suspension was diluted in complete medium to reach a 2× working concentration and added to the J774 macrophages 1:1 (final R848 working concentration 0.1 μg/ml; final NP concentration: 15.8 μg/ml NPa, 82.6 μg/ml NPb). u-NP (unloaded) and DiO-NP were used at the same concentrations as the respective R848-NP unless indicated otherwise.

2.7. Cytotoxicity assay

J774 macrophages (5×10^4 cells/well) were exposed for 24 h to u-NPs or R848-NP. Staurosporine (0.1 μm) was used as a positive control. Cells were stained with annexin V in annexin V buffer (both from Biolegend). Propidium iodide (PI; 0.5 mg/ml, Sigma) was added automatically at 1:100 dilution before acquisition by the MACSquant Analyzer 10 flow cytometer (Miltenyi Biotec). Data were analyzed using FlowJo software.

2.8. NP uptake in J774 cells

For flow cytometry analysis, J774 macrophages (5×10^4 cells/well) were exposed for 24 h to DiO-NP at 4 °C or 37 °C and resuspended in FACS buffer (PBS, 0.5% bovine serum albumin (BSA) and 5 mM EDTA, PAA). Zombie violet (Biolegend) was used to exclude dead cells. For confocal microscopy, J774 cells (5×10^5 cells/ml) were incubated in 300 μl with 4 μg/ml NP for 10 h in complete medium. 75 nM LysoTracker DND22 (blue; Invitrogen) were used for lysosomal staining according to manufacturer's protocol. Cells were visualized using a confocal microscope (Zeiss 710 Meta, 63× oil immersion objective).

2.9. Immune activation

J774 macrophages (5×10^4 cells/well) were incubated with NP-R848 (0.1 μg/ml of R848) for 24 h and resuspended in FACS buffer. Free R848 was used as positive control. Cells were stained with Zombie violet and incubated with Fc block True Stain fcX CD16/32 (Biolegend) for 15 min before addition of the following antibodies: MHCII (APC-Cy7, clone M5/114.15.2), CD86 (PE, clone GL-1), CD11b (PE-Cy7, clone M1/70) (all Biolegend). Data was acquired by MACSquant Analyzer and analyzed using FlowJo software. Interleukin-6 (IL-6) was determined in the cell culture supernatant using Mouse IL-6 ELISA MAX kit (Biolegend) according to the manufacturer's protocol. Absorbance at 570 nm was measured and subtracted from the absorbance at 450 nm by Infinite 200 PRO plate-reader (TECAN).

2.10. Uptake into splenocytes

Splenocytes were isolated from C57BL/6 mice and red blood cell lysis was performed (BD Pharm Lyse, BD). Cells were resuspended in T-cell medium: RPMI1640 (PAA), 2 mmol/ml L-glutamine (PAA), 1 IU/ml Penicillin (PAA), 100 mg/ml streptomycin (PAA), 0.1 mm non-essential amino acid (PAA), 1 mm sodium pyruvate and 25 μM beta-mercapto ethanol (both life technologies). Splenocytes (10^6 cells/well in a 24-well plate) were incubated for 2 h with DiO-NP at the standard working concentration (15.8 μg/ml NPa, 82.6 μg/ml NPb) or at 10× working concentration. This short incubation time was selected due to the short half-life in culture of some primary cells. Cells were washed twice with PBS before flow cytometry staining with Zombie violet, incubation with Fc block for 15 min before addition of the following antibodies: CD11b (APC, clone M1/70), CD19 (APC-Cy7, clone 6D5), CD3 (PB, clone 17A2) and CD11c (PE, clone N418) (all from Biolegend). Data was acquired by flow cytometry as described above.

2.11. Biodistribution

500 μg of DiO-NP in 100 μl PBS were injected *s.c.* close to the inguinal space in C57BL/6 mice (Janvier Labs). 24 h after injection, spleen and lymph nodes were isolated and single cell suspensions were prepared. The inguinal lymph nodes ipsilateral to the injection (draining lymph nodes), and inguinal lymph nodes contralateral to the injection (non-draining lymph nodes) were isolated. Lymph nodes were cut into 3–4 pieces before passing through a 40 μm cell strainer. After centrifugation, single cell suspensions were resuspended in medium and counted. Erythrocyte lysis was performed for spleen (BD Pharm Lyse). Cells were stained with Zombie violet and incubated with Fc block for 15 min before addition of the following antibodies: CD11b (Pe-Cy7, Clone M1/70), B220 (PB, Clone RA3-6B2), CD3 (PerCP, clone 17A2) and CD11c (APC-Cy7, clone N418) (all from Biolegend) before flow cytometry analysis.

3. Results

3.1. NP synthesis and characterization

While the PLGA polymer was commercially available, mPEG-PLA was synthesized under bulk conditions *via* a ring-opening polymerization (ROP) of DL-lactide, using mPEG 2000 as the initiator and stannous octoate as the catalyst. By ^{1}H NMR spectroscopy it was possible to assess the molecular weight of the synthesized polymer by calculating the ratio of protons corresponding to mPEG moiety *vs* protons corresponding to polylactic acid moiety. A molecular weight of 8 kDA was

4

A
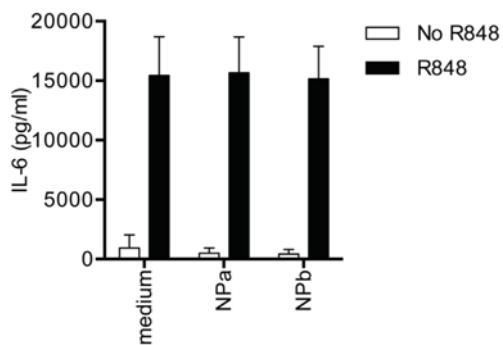
B
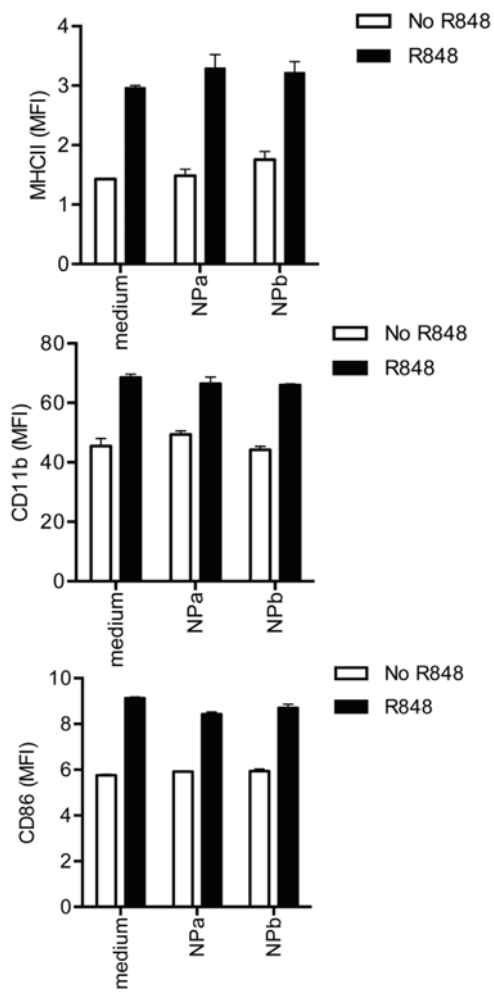
Fig. 4. R848 released by NP efficiently activates macrophages.
J774 macrophages were exposed for 24 h to u-NP or R848-NP. (A) IL-6 levels in supernatant were measured by ELISA. Each bar represents mean ± SEM of 4 independent experiments performed in quadruplicate. (B) Cell surface expression of MHCII, CD11b and CD86 was measured by flow cytometry. Medium: incubation condition without NP, without R848 (white bar) or with free R848 (black bar). Each bar represents mean ± SD of one experiment performed in triplicate. Data are representative of 3 independent experiments.

determined.

Batches of NP constituted of a 67/33 mass blend of PLGA and mPEG-PLA (NPa) or 100% mPEG-PLA (NPb) were then synthesized by a solvent-evaporation method. These NP were either loaded with R848 as the active molecule (R848-NP), DiO as a fluorescent probe (DiO-NP) or unloaded (u-NP). Particles had a mean size ranging from 154 to

278 nm. Their zeta potential ranged from −10 to −25 mV. Table 1 summarizes the principal characteristics of the different batches. Scanning electron microscopy showed spherical and homogeneous shape of the particles both for NPa and NPb (Fig. 1). However, although NPb are well dispersed in the aqueous medium, they appear as merging entities when deposited on the slabs (Fig. 1B) due to the high percentage of hydrophilic PEG moiety.

3.2. NP are taken up by a macrophage cell line

To examine whether NP were internalized by antigen-presenting cells, we used the well-characterized macrophage cell line J774. J774 cells were exposed to DiO-NPa and DiO-NPb for 24 h and NP uptake was assessed by flow cytometry. Both NPa and NPb were efficiently taken up by macrophages at 37 °C, as we measured over 40% DiO-positive cells for NPa and approximately 90% DiO-positive cells for NPb (Fig. 2A and B). NP were also exposed to J774 macrophages for 24 h at 4 °C, a temperature at which many active intracellular processes are decreased (Sokolova et al., 2013). At this temperature, the amount of DiO-positive cells was strongly reduced for both NPa and NPb, indicating that a major part of the NP is actively taken up at 37 °C. J774 cells incubated with DiO-NP were also examined by confocal microscopy. DiO-NP (green) were observed to accumulate in vesicles inside the cells and colocalized with LysoTracker, an endosomal marker (blue) (Fig. 2C). Thus, our results show that NPa and NPb are readily taken up by macrophages.

3.3. NP do not affect macrophage viability

The impact of NPa and NPb on the viability of J774 macrophages was examined by flow cytometry with annexin V/PI staining. These NP did not affect cell viability after 24 h of exposure, as there was no significant change in the proportion of live annexin V/PI double-negative cells after incubation (Fig. 3). The impact on cell viability was also assessed for R848-NPa and R848-NPb (Fig. 3C). No decrease in cell viability was observed after incubation with these particles. Thus, neither NPa nor NPb affect the viability of macrophages, both with and without R848 cargo.

3.4. R848-loaded NP activate macrophages

The imidazoquinoline R848 is a pharmacological immunostimulant that activates the Toll-like receptor 7, which is present in the endosome of myeloid immune cells such as macrophages (Heil et al., 2003). To assess the immune-activating effect of R848 delivered by NP, we determined the amount of the pro-inflammatory cytokine interleukin 6 (IL-6) secreted by J774 macrophages after exposure to R848-NP. When J774 macrophages were exposed to u-NP, no IL-6 was produced, indicating that these NP are not pro-inflammatory by themselves. In contrast, J774 cells exposed to free R848 produced high amounts of IL-6, as expected (Fig. 4A). J774 exposed to R848-NP produced IL-6 in high amounts, similar to the J774 cells exposed to free R848. Furthermore, activation markers were measured on J774 cells by flow cytometry. R848-NPa and R848-NPb enhanced the surface expression of the activation markers MHC-II, CD11b and CD86 to a similar extent as free R848 (Fig. 4B). In contrast, u-NP did not significantly enhance the expression of these markers. Thus, unloaded NP do not cause activation of macrophages, whereas R848-NP lead to a strong activation of macrophages.

3.5. NP are taken up by primary immune cells

The expression of the Toll-like receptor 7 in the organism is mainly restricted to immune cells of the myeloid lineage, including macrophages, monocytes and dendritic cells, and to B lymphocytes. To determine whether these primary cells take up NPa and NPb, we exposed
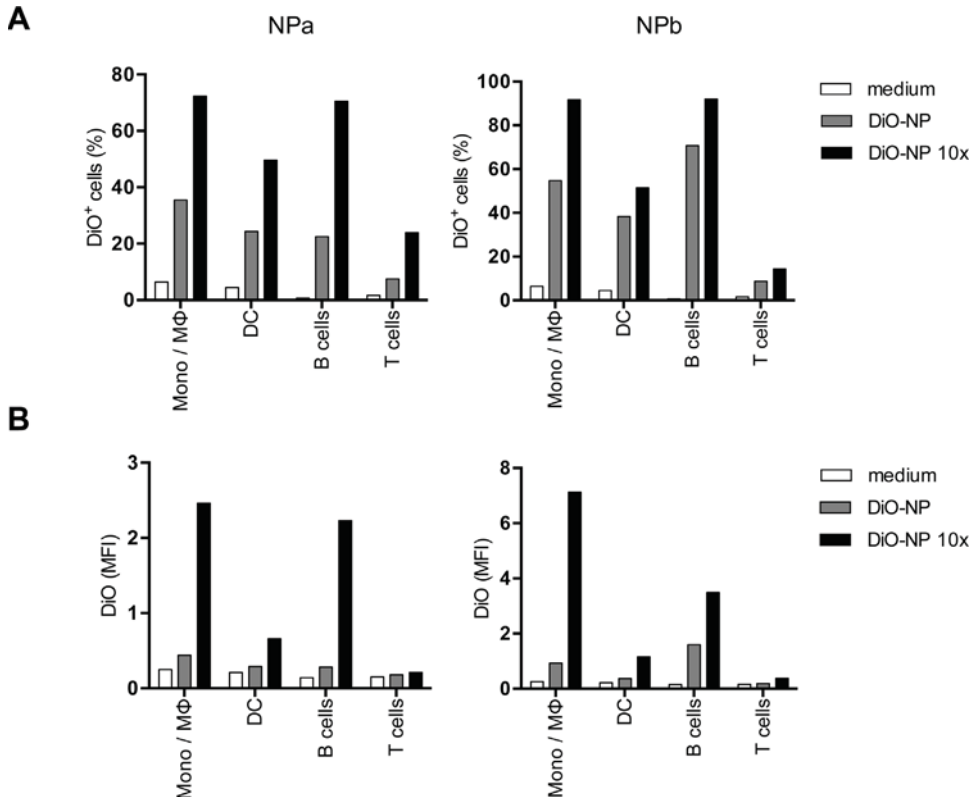
Fig. 5. NP are efficiently taken up by primary antigen-presenting cells.
Freshly isolated splenocytes were exposed for 2 h to DiO-NP before flow cytometry analysis. (A) Percentage of DiO-positive cells within the indicated cell populations: monocytes/macrophages (mono/Mϕ) (CD11b + CD11c −), dendritic cells (DC) (CD11b + CD11c +), B lymphocytes (CD19 +), T cells (CD3 +) and (B) Mean fluorescence intensity (MFI) of DiO in the indicated cell populations. Data are representative of 2 independent experiments.
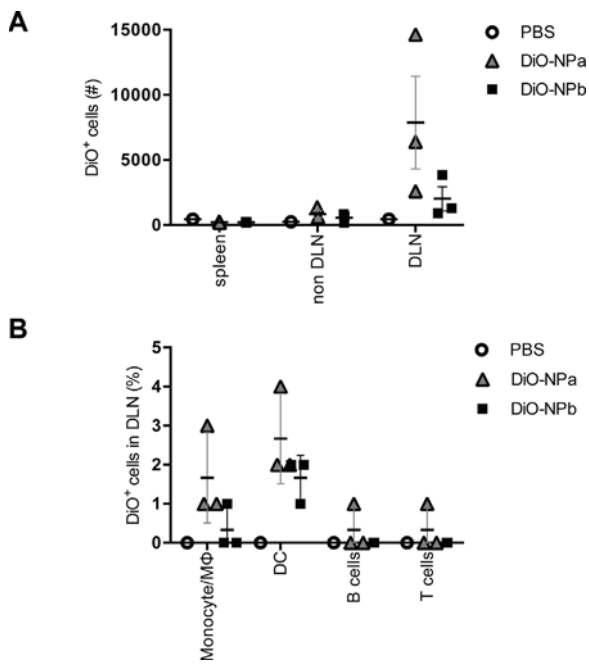
Fig. 6. *In vivo*, NP accumulate in antigen-presenting cells of the draining lymph nodes. 500 μg DiO-NP were injected *s.c.* into the flank of C57BL/6 mice (n = 3). PBS (no NP) was used as negative control (n = 1). 24 h after injection, cells from the spleen, the non-draining lymph nodes (non-DLN) and the draining lymph nodes (DLN) were isolated for flow cytometry analysis. (A) Number of DiO-positive cells in the indicated organs. (B) Percentage of DiO-positive cells in DLN within the indicated cell populations: Monocytes/macrophages (mono/Mϕ) (CD11b + CD11c −), dendritic cells (DC) (CD11b+CD11c +), B lymphocytes (CD19 +), T cells (CD3 +). Data are representative of 2 independent experiments.

freshly isolated murine splenocytes to DiO- NP for 2 h. The spleen contains a variety of immune cells, in particular B and T lymphocytes and a mixture of myeloid cells. Our results confirm that also freshly isolated CD11b-positive monocytes and macrophages took up NPa and NPb. Indeed, at the higher concentration of 1 μg/ml NP, approximately 70% and 90% of monocytes/macrophages were DiO-positive for DiO-NPa and DiO-NPb, respectively (Fig. 5A). Approximately 50% of dendritic cells (DC) took up both types of NP. We observed that NP are also taken up by lymphocytes, with 70–90% of DiO-positive B cells and 10–20% of DiO-positive T cells. We further examined the mean fluorescence intensity (MFI) of the different cell populations (Fig. 5B). The cells with the highest MFI were the monocytes/macrophages and the B cells, confirming that these populations take up the most NP.

3.6. NP are targeted to the lymph nodes

Since the initiation of adaptive immune responses occurs in the lymph nodes, it is of great importance that NP serving as delivery system for immune activators should be transported to these organs. To examine whether this was the case for NPa and NPb, we injected DiO-NP subcutaneously in mice and isolated spleen and draining and non-draining lymph nodes 24 h after injection. We found DiO-positive cells mainly in the draining lymph nodes, very few DiO-positive cells in non-draining lymph nodes and none in the spleen (Fig. 6A). We further investigated which cell types took up NPs within the draining lymph nodes. Both DiO-NPa and DiO-NPb were mainly taken up by dendritic cells (DC) and the monocyte/macrophage CD11b+ population (Figs. 6B and S1). These cell types are antigen-presenting cells and are instrumental for initiating immune responses. In addition, both these cell types express the Toll-like receptor 7. Thus, NP are targeted to the draining lymph nodes following *s.c.* application.

4. Discussion

Imidazoquinolines including R848 can generate highly effective

6

antitumoral responses (Kobold et al., 2014). However, these small molecules also induce inflammatory responses with high serum levels of proinflammatory cytokines when applied systemically. Indeed, even subcutaneous application of R848 leads to a rapid increase of the cytokines IFNα and IL-6 in the serum (Bourquin et al., 2011). Since these unspecific and generalized inflammatory responses can result in dose-limiting toxicity (Kobold et al., 2014), it is of great therapeutic interest to develop particulate delivery systems that may focus the immune-activating effect of these molecules to the target tissues.

Here, we successfully encapsulated R848 in either mPEG-PLA or PLGA/mPEG-PLA nanoparticles. Interestingly, the encapsulation rate was higher when PLGA was present in the formulation (8.36 μg/mg of NP vs 0.74 μg/mg of NP). The exclusive presence of the PEG hydrophilic moieties in R848-NPb batches resulted in lower affinity of the drug to the polymer matrix leading therefore to lower encapsulation rates. In the literature, several studies relate the encapsulation of R848 or analogues in polymer nanoparticles either alone or co-encapsulated with antigens or adjuvants (Cruz et al., 2012; Ilyinskii et al., 2014; Kasturi et al., 2017, 2011; Seth et al., 2017; Tacken et al., 2011; Tel et al., 2013). When encapsulation rates are given by the authors, the values are ranging from 1.2 to 6.4 μg/mg of NP. However, in these specific cases, co-encapsulation of resiquimod with antigens or adjuvants in NP made of RG502H as PLGA is discussed. Only Seth et al. report an encapsulation rate of 11.1 μg/mg while loading a resiquimod analogue, gardiquimod, alone in PLGA NP. Comparison with our data is difficult as preparation methods and materials are different. It is well known that the molecular weight and the PLA/PLGA ratio are crucial factors in the encapsulation efficiency. However, we assume that the encapsulation efficiencies observed herein are in the same order of magnitude as those observed in the literature. Pure mPEG-PLA nanoparticles (NPb) were smaller than mixed polymer nanoparticles (NPa). This observation is likely related to the combined action of 1) the more amphiphilic nature of the pegylated polymer and 2) its lower molecular weight. Indeed, we observed that by fixing the molecular weight of the polymer, the only addition of an mPEG moiety does not lead to a change in the size of the nanoparticles.

Both TLR7 ligand R848-loaded mPEG-PLA NP and PLGA/mPEG-PLA NP were readily taken up by antigen-presenting cells such as macrophages and dendritic cells both in vitro and in vivo (Figs. 2, 5 and 6). Importantly, the R848 cargo could induce immune activation of these cells, demonstrating its accessibility to the immune system (Fig. 3). We observed similar levels of activation in cell culture with R848-loaded NP and with the same amount of free R848. Depending on the type of NP used as carrier, others have seen similar results or even reduced activation in vitro with NP-delivered R848 (Tacken et al., 2011; Cruz et al., 2012; Ilyinskii et al, 2014). The addition of molecules to the surface of the NP that specifically target dendritic cells may further improve the uptake of the particles and the immunostimulatory activity of R848 cargo, as shown with polymer-based NP decorated with anti-DC-SIGN antibodies (Cruz et al., 2012). The unloaded particles did not show any unspecific proinflammatory effects, demonstrating the absence of relevant levels of endotoxin, and none of the NP tested showed cytotoxicity, highlighting their biocompatibility.

The use of mPEG-PLA or PLGA/mPEG-PLA NP allows delivery of R848 specifically to antigen-presenting cells. In vitro, these NP are taken up by B cells, dendritic cells, monocytes and macrophages, whereby monocytes/macrophages seem to take up larger amounts of particles (Amoozgar and Goldberg, 2015). Following subcutaneous injection, the NP are found within the draining lymph nodes both in dendritic cells and in macrophages. These cells are responsible for initiating the T cell-mediated immunity that is crucial for anti-tumor efficacy, and are therefore the prime therapeutic target (Chen and Mellman, 2013). Considering the size of the particles (> 150 nm), it is probable that the NP were taken up by the antigen-presenting cells at the site of injection and carried to the lymph nodes, rather than reaching the nodes by passive diffusion through the lymph, as would be the case for smaller NP (Irvine et al., 2013). Little uptake is seen by B cells, which do not reside in subcutaneous areas.

Targeting TLR7 agonists directly to the lymph nodes offers several advantages, since this can focus immune activation to the injection site and the draining lymph node. This targeting has been shown to enhance cytotoxic T-cell responses when the TLR7 agonist is applied together with antigen in the context of vaccination (Jewell et al., 2011; Nuhn et al., 2016). In addition, lymph node targeting of TLR ligands can reduce systemic levels of proinflammatory cytokines (Bourquin et al., 2008). We propose that mPEG-PLA and PLGA/mPEG-PLA nanoparticles represent an attractive and safe delivery system to target small molecule TLR7 agonists to lymph nodes, allowing a focused immune response that may be of benefit for anticancer immunotherapy.

Appendix A. Supplementary data

Supplementary material related to this article can be found, in the online version, at doi:https://doi.org/10.1016/j.ijpharm.2017.11.031

References

Allémann, E., Gurny, R., Doelker, E., 1993. Drug-loaded nanoparticles: preparation methods and drug targeting issues. Eur. J. Pharm. Biopharm. 39, 173–191.

Amoozgar, Z., Goldberg, M.S., 2015. Targeting myeloid cells using nanoparticles to improve cancer immunotherapy. Adv. Drug Deliv. Rev. 91, 38–51.

Anz, D., Koelzer, V.H., Moder, S., Thaler, R., Schwerd, T., Lahl, K., Sparwasser, T., Besch, R., Poeck, H., Hornung, V., Hartmann, G., Rothenfusser, S., Bourquin, C., Endres, S., 2010. Immunostimulatory RNA blocks suppression by regulatory T cells. J. Immunol. 184, 939–946.

Bourquin, C., Anz, D., Zwiorek, K., Lanz, A.L., Fuchs, S., Weigel, S., Wurzenberger, C., von der Borch, P., Golic, M., Moder, S., Winter, G., Coester, C., Endres, S., 2008. Targeting CpG oligonucleotides to the lymph node by nanoparticles elicits efficient antitumoral immunity. J. Immunol. 181, 2990–2998.

Bourquin, C., Hotz, C., Noerenberg, D., Voelkl, A., Heidegger, S., Roetzer, L.C., Storch, B., Sandholzer, N., Wurzenberger, C., Anz, D., Endres, S., 2011. Systemic cancer therapy with a small molecule agonist of toll-like receptor 7 can be improved by circumventing TLR tolerance. Cancer Res. 71, 5123–5133.

Bourquin, C., Schmidt, L., Lanz, A.L., Storch, B., Wurzenberger, C., Anz, D., Sandholzer, N., Mocikat, R., Berger, M., Poeck, H., Hartmann, G., Hornung, V., Endres, S., 2009. Immunostimulatory RNA oligonucleotides induce an effective antitumoral NK cell response through the TLR7. J. Immunol. 183, 6078–6086.

Chen, D.S., Mellman, I., 2013. Oncology meets immunology: the cancer-immunity cycle. Immunity 39, 1–10.

Cruz, L.J., Tacken, P.J., Pots, J.M., Torensma, R., Buschow, S.I., Figdor, C.G., 2012. Comparison of antibodies and carbohydrates to target vaccines to human dendritic cells via DC-SIGN. Biomaterials 33, 4229–4239.

Dumitru, C.D., Antonysamy, M.A., Gorski, K.S., Johnson, D.D., Reddy, L.G., Lutterman, J.L., Piri, M.M., Proksch, J., McGurran, S.M., Egging, E.A., Cochran, F.R., Lipson, K.E., Tomai, M.A., Gullikson, G.W., 2009. NK1.1 + cells mediate the antitumor eVects of a dual toll-like receptor 7/8 agonist in the disseminated B16-F10 melanoma model. Cancer Immunol. Immunother. 58, 575–587.

Fahr, A., Liu, X., 2007. Drug delivery strategies for poorly water-soluble drugs. Expert Opin. Drug Deliv. 4, 403–416.

Goldinger, S.M., Dummer, R., Baumgaertner, P., Mihic-Probst, D., Schwarz, K., Hammann-Haenni, A., Willers, J., Geldhof, C., Prior, J.O., Kundig, T.M., Michielin, O., Bachmann, M.F., Speiser, D.E., 2012. Nano-particle vaccination combined with TLR-7 and -9 ligands triggers memory and effector CD8(+) T-cell responses in melanoma patients. Eur. J. Immunol. 42, 3049–3061.

Heil, F., Ahmad-Nejad, P., Hemmi, H., Hochrein, H., Ampenberger, F., Gellert, T., Dietrich, H., Lipford, G., Takeda, K., Akira, S., Wagner, H., Bauer, S., 2003. The Toll-like receptor 7 (TLR7)-specific stimulus loxoribine uncovers a strong relationship within the TLR7, 8 and 9 subfamily. Eur. J. Immunol. 33, 2987–2997.

Hotz, C., Treinies, M., Mottas, I., Rotzer, L.C., Oberson, A., Spagnuolo, L., Perdicchio, M., Spinetti, T., Herbst, T., Bourquin, C., 2016. Reprogramming of TLR7 signaling enhances antitumor NK and cytotoxic T cell responses. Oncoimmunology 5, e1232219.

Ilyinskii, P.O., Roy, C.J., O'Neil, C.P., Browning, E.A., Pittet, L.A., Altreuter, D.H., Alexis, F., Tonti, E., Shi, J., Basto, P.A., Iannacone, M., Radovic-Moreno, A.F., Langer, R.S., Farokhzad, O.C., von Andrian, U.H., Johnston, L.P., Kishimoto, T.K., 2014. Adjuvant-carrying synthetic vaccine particles augment the immune response to encapsulated antigen and exhibit strong local immune activation without inducing systemic cytokine release. Vaccine 32, 2882–2895.

Iribarren, K., Bloy, N., Buque, A., Cremer, I., Eggermont, A., Fridman, W.H., Fucikova, J., Galon, J., Spisek, R., Zitvogel, L., Kroemer, G., Galluzzi, L., 2016. Trial watch: immunostimulation with toll-like receptor agonists in cancer therapy. Oncoimmunology 5, e1088631.

Irvine, D.J., Swartz, M.A., Szeto, G.L., 2013. Engineering synthetic vaccines using cues from natural immunity. Nat. Mater. 12, 978–990.

Iwasaki, A., Medzhitov, R., 2015. Control of adaptive immunity by the innate immune system. Nat. Immunol. 16, 343–353.

Jewell, C.M., Lopez, S.C., Irvine, D.J., 2011. In situ engineering of the lymph node microenvironment via intranodal injection of adjuvant-releasing polymer particles. Proc. Natl. Acad. Sci. U. S. A. 108, 15745–15750.

Kasturi, S.P., Kozlowski, P.A., Nakaya, H.I., Burger, M.C., Russo, P., Pham, M., Kovalenkov, Y., Silveira, E.L., Havenar-Daughton, C., Burton, S.L., Kilgore, K.M., Johnson, M.J., Nabi, R., Legere, T., Sher, Z.J., Chen, X., Amara, R.R., Hunter, E., Bosinger, S.E., Spearman, P., Crotty, S., Villinger, F., Derdeyn, C.A., Wrammert, J., Pulendran, B., 2017. Adjuvanting a simian immunodeficiency virus vaccine with toll-like receptor ligands encapsulated in nanoparticles induces persistent antibody responses and enhanced protection in TRIM5alpha restrictive *Macaques*. J. Virol. 91 e01844-16.

Kasturi, S.P., Skountzou, I., Albrecht, R.A., Koutsonanos, D., Hua, T., Nakaya, H.I., Ravindran, R., Stewart, S., Alam, M., Kwissa, M., Villinger, F., Murthy, N., Steel, J., Jacob, J., Hogan, R.J., Garcia-Sastre, A., Compans, R., Pulendran, B., 2011. Programming the magnitude and persistence of antibody responses with innate immunity. Nature 470, 543–547.

Kobold, S., Wiedemann, G., Rothenfusser, S., Endres, S., 2014. Modes of action of TLR7 agonists in cancer therapy. Immunotherapy 6, 1085–1095.

Kranz, L.M., Diken, M., Haas, H., Kreiter, S., Loquai, C., Reuter, K.C., Meng, M., Fritz, D., Vascotto, F., Hefesha, H., Grunwitz, C., Vormehr, M., Husemann, Y., Selmi, A., Kuhn, A.N., Buck, J., Derhovanessian, E., Rae, R., Attig, S., Diekmann, J., Jabulowsky, R.A., Heesch, S., Hassel, J., Langguth, P., Grabbe, S., Huber, C., Tureci, O., Sahin, U., 2016. Systemic RNA delivery to dendritic cells exploits antiviral defence for cancer immunotherapy. Nature 534, 396–401.

Leroux, J.-C., Allémann, E., De Jaeghere, F., Doelker, E., Gurny, R., 1996. Biodegradable nanoparticles—from sustained release formulations to improved site specific drug delivery. J. Control. Release 39, 339–350.

Nishiya, T., DeFranco, A.L., 2004. Ligand-regulated chimeric receptor approach reveals distinctive subcellular localization and signaling properties of the Toll-like receptors. J. Biol. Chem. 279, 19008–19017.

Nuhn, L., Vanparijs, N., De Beuckelaer, A., Lybaert, L., Verstraete, G., Deswarte, K., Lienenklaus, S., Shukla, N.M., Salyer, A.C.D., Lambrecht, B.N., Grooten, J., David, S.A., De Koker, S., De Geest, B.G., 2016. pH-degradable imidazoquinoline-ligated nanogels for lymph node-focused immune activation. Proc. Natl. Acad. Sci. U. S. A. 113, 8098–8103.

Papakostas, D., Stockfleth, E., 2015. Topical treatment of basal cell carcinoma with the immune response modifier imiquimod. Future Oncol. 11, 2985–2990.

Riehemann, K., Schneider, S.W., Luger, T.A., Godin, B., Ferrari, M., Fuchs, H., 2009. Nanomedicine–challenge and perspectives. Angew. Chem. Int. Ed. Engl. 48, 872–897.

Seth, A., Lee, H., Cho, M.Y., Park, C., Korm, S., Lee, J.-Y., Choi, I., Lim, Y.T., Hong, K.S., 2017. Combining vasculature disrupting agent and toll-like receptor 7/8 agonist for cancer therapy. Oncotarget 8, 5371–5381.

Sokolova, V., Kozlova, D., Knuschke, T., Buer, J., Westendorf, A.M., Epple, M., 2013. Mechanism of the uptake of cationic and anionic calcium phosphate nanoparticles by cells. Acta Biomater. 9, 7527–7535.

Spinetti, T., Spagnuolo, L., Mottas, I., Secondini, C., Treinies, M., Ruegg, C., Hotz, C., Bourquin, C., 2016. TLR7-based cancer immunotherapy decreases intratumoral myeloid-derived suppressor cells and blocks their immunosuppressive function. Oncoimmunology 5, e1230578.

Tacken, P.J., Zeelenberg, I.S., Cruz, L.J., van Hout-Kuijer, M.A., van de Glind, G., Fokkink, R.G., Lambeck, A.J., Figdor, C.G., 2011. Targeted delivery of TLR ligands to human and mouse dendritic cells strongly enhances adjuvanticity. Blood 118, 6836–6844.

Tel, J., Sittig, S.P., Blom, R.A., Cruz, L.J., Schreibelt, G., Figdor, C.G., de Vries, I.J., 2013. Targeting uptake receptors on human plasmacytoid dendritic cells triggers antigen cross-presentation and robust type I IFN secretion. J. Immunol. 191, 5005–5012.

Zeisser-Labouèbe, M., Lange, N., Gurny, R., Delie, F., 2006. Hypericin-loaded nanoparticles for the photodynamic treatment of ovarian cancer. Int. J. Pharm. 326, 174–181.